Limited Data Tomography: A Model of Sonar Technology

Claire Callon† and Project Advisor: Eric Todd Quinto‡

Abstract. This article examines a sonar model where the source and detector are at the same point. The goal is to reconstruct objects in the ocean by integrating over the curves generated by the sonar source. Moving the sonar source along different curves or lines develops reconstructions with a varying amount of visible singularities and unique artifacts. This article explores the artifacts produced from object reconstructions and the effectivity of these reconstructions in depicting the object. Previous principles proved by Dr. Quinto and others explain some of the artifacts, but this article also discusses a new type of artifact that we found.

1. Introduction. In this article, we verify principles that Dr. Quinto and others found for X-ray CT, e.g., [2, 7], and for sonar in [4, 8]. We generated reconstructions for a different limited data tomography problem, to do with sonar technology, to verify these principles and also found elements of these reconstructions that have yet to be justified mathematically. In our limited data tomography problem, we examine how a sonar source is capable of reconstructing objects in the ocean when the sonar source is traveling among different paths. For references on tomography and wave equation imaging in general, see e.g., [6, 3, 11].

In our research, we mostly examined elements that appeared in the reconstruction that did not appear in the initial reconstruction region, called artifacts. We verified that end-of-data set artifacts occur, which was proven previously in a closely related limited data tomography problem for the spherical transform [4]. We also verified that mirror point artifacts do occur in filtered backprojection, which was suggested but not shown in another article [1]. We discovered a new type of artifact, later named 'stationary point artifacts,' discussed in this article.

The justification of our observations for this limited data tomography problem involves microlocal analysis and the Fourier transform (e.g., [5]). However, for the purposes of developing the reconstructions, various calculus and data approximation techniques can be used.

In this article, we first illustrate how to generate a reconstruction mathematically when the sonar source is simply traveling along a straight line. We then move into more complicated reconstructions when the sonar source is traveling along a curve. We conduct artifact analysis on these reconstructions throughout the paper to verify the artifacts mentioned above, as well as discuss the new artifact found.

2. Problem 1. The first limited data tomography provides the groundwork for more complicated reconstructions. In this problem, the source of the sonar waves is along the ocean's surface. The sonar waves' curves must be integrated over to reconstruct an object in the ocean. The limited data in both the centers and radii of the sonar waves affect the effectiveness of the object reconstruction. An explanation of the math behind developing these object reconstructions follows.

†Amherst College, Amherst, MA 01002 (ccallon25@amherst.edu).
‡Department of Mathematics, Tufts University, Medford, MA (todd.quinto@tufts.edu).

2.1. Math Behind Problem 1. The reconstruction region must first be defined to begin an object reconstruction. One of the simplest objects to reconstruct is a circle, but the reconstruction method can be generalized to any shape. For this problem, the centers of the sonar waves, or circles, will have centers of $(s, 0)$ where s is limited from $(-10, 10)$. Each circle will have an associated radius of r, where r is limited from $(0, 10)$.

When integrating over these circles, the characteristic function of an object will be used. The characteristic function represents the density of the object. From here on, the characteristic function will be referred to as:

$$f(x,y) = \begin{cases} 1 & (x-c_1)^2 + (y-c_2)^2 \le R^2 \\ 0 & \text{otherwise} \end{cases} \tag{1}$$

In this case, the object is a disk centered at (c_1, c_2) with radius $R > 0$.

To integrate over the circles, each circle is first parameterized, and the parameterization is plugged into the characteristic function described above. For a circle centered at (x_0, y_0) with radius r, the integral is:

$$Rf((x_0,y_0),r) := \int_0^{2\pi} f(x_0 + r * \cos(\theta), y_0 + r * \sin(\theta)) * r \; d\theta. \tag{2}$$

In this problem, $x_0 = s \in \mathbb{R}$, and y_0 is always 0 since the source of sonar waves is on the ocean's surface (i.e., the line $y = 0$). Then one only needs to integrate over the half-circle in the ocean. The trapezoidal rule is then used on the integral in (2) to generate data

$$D(s_i, r_j) = Rf((s_i, 0), r_j) \tag{3}$$

at points (s_i, r_j), where s_i are evenly spaced points in $[-10, 10]$ and r_j are evenly spaced points in $[0, 10]$ when the circle being integrated over passes through the object being reconstructed. In this case, D forms a matrix produced from the trapezoidal rule data, (3), where the first index contains the centers of the circles and the second index contains the radii of the circles. I will call this matrix trapezoidal rule matrix.

Then, the second derivative of the data is approximated using the central second difference. The second derivative in s is needed in some of our reconstructions because it clearly highlights the object's boundaries. The boundaries are evident in the second derivative because the second derivative yields either largely positive or largely negative values on the data corresponding to the boundaries of the object [9]. The formula for the central second difference is as follows:

$$\frac{\partial^2}{\partial r^2} D(s_i, r_j) \approx \frac{D(s_i, r_{j+1}) - 2 * D(s_i, r_j) + D(s_i, r_{j-1})}{(\Delta(r))^2} \tag{4}$$

In this case, the results of (4) form a matrix that I will call the central second difference matrix.

After obtaining both the data from the trapezoidal rule, (3), and the central second difference, (4), the backprojection produces an image (reconstruction) of the object. The backprojection at a point $\bar{x}$ integrates data over all the circles in the data set that contain

$\bar{x}$. The continuous backprojection is given in equation (6) below. In problem 1, the curve of sources is $\gamma(s) = (s, 0)$. Backprojection can use either the data from the trapezoidal rule, $D(s_i, r_j)$, or the central second difference as in (4). However, a backprojection that uses the data from the central second difference produces a reconstruction that emphasizes the object's boundaries more. As $\bar{x}$ gets closer to the object, the backprojection data will yield either larger positive or negative values, which helps produce an effective reconstruction.

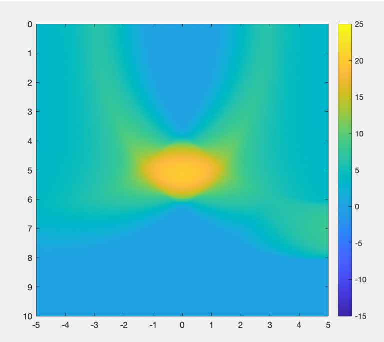

(a) Backprojection reconstruction using trapezoidal rule matrix

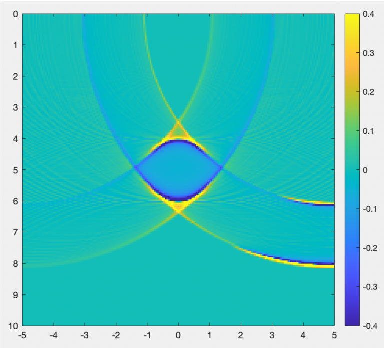

(b) Backprojection reconstruction using central second difference matrix

Figure 1: Reconstructions with sonar source and receiver on the surface.

To integrate over all circles that go through a point $\bar{x}$, all circles with centers $(s, 0)$ with associated radii are found, where s is limited to $[-5, 5]$. The associated radii are found through using the distance formula between the point $\bar{x}$ and $(s, 0)$. The integration of these circles is again carried out through the trapezoidal rule using data from the matrices produced by the trapezoidal rule and the central second difference. The values inputted into these matrices are the center s value and the associated radius, r. However, since r is being calculated through the distance formula, it could potentially not align with an r value in one of the matrices. To resolve this issue, linear interpolation must be used. For example, to approximate the data for r that is between $[r_{j-1}, r_j]$, where j refers to the index for the matrix, the formula below is used:

$$B(s_i, r) = D(s_i, r_{j-1}) + (r - r_{j-1}) * \frac{D(s_i, r_j) - D(s_i, r_{j-1})}{r_j - r_{j-1}} \tag{5}$$

In this case, matrix B will refer to the matrix containing the backprojection values. Once a value for an arbitrary r is approximated, the trapezoidal rule integration can take place to complete the backprojection data.

Above is an example of a backprojection reconstruction where the object is a circle centered at $(0, 5)$ with a radius of 1. From the images above, it is clear that the central second difference matrix produces a better reconstruction, so this is the matrix that will be used in most reconstructions.

2.2. Definitions and Principles. We will now introduce some definitions and principles that are essential to analyzing the reconstructions. First, the definitions:

Singularity
: A point at which the density function of the object is not differentiable or infinitely differentiable

Visible Singularity
: A singularity in the object that appears in the reconstruction.

Invisible Singularity
: A singularity in the object that does not appear in the reconstruction

Artifact
: A singularity in the reconstruction that is not in the object.

Second, the principles found in [9, 4, 10]:

Principle 2.1. (a) If a boundary of a feature of the body is tangent to a circle in a limited data set, then that boundary should be easy to reconstruct from that limited data. Such boundaries are called visible boundaries (from this limited data).
(b) If a boundary is not tangent to any circle in a limited data set, then that boundary should be difficult to reconstruct from the limited data. Such boundaries are called invisible boundaries (from this limited data).

Principle 2.2. Artifacts can occur on circles at the ends of the data set (e.g., at $(s_{\min}, 0)$ and $(s_{\max}, 0)$ for Problem 1) that are tangent to some feature of the object.

The principle applies to this limited data problem by [4]. We can expect to see artifact circles occur when the centers, $(s, 0)$, are at the end of the data set. These definitions and principles can be used to examine the first reconstruction displayed.

2.3. Examination of a Reconstruction from Problem 1. We will now explain the above-mentioned definitions and principles regarding the reconstruction labeled 1b. The visible singularities of the object are where the circle is reconstructed well, i.e., the top and bottom of the circle. According to principle 2.1, this is because there are circles in the data set that are tangent to the top and the bottom of the object since the source of sonar is on the line $y_0 = 0$. On the other hand, the left and right of the object are not reconstructed well because the backprojection generates vertices (the points at the left- and right-ends of the object in the reconstruction) as opposed to circular arcs. The left and right circular arcs of the object are called invisible singularities, and they occur because there are no circles in the data set that are tangent to these boundaries of the object.

The larger circular arcs generated in the reconstruction are called artifacts because they are not a part of the object. However, these artifacts can be explained by principle 2.2. In figure 2, it is clear that these artifacts are generated by circles centered on the endpoints of s.

By symmetry, the other artifacts in this reconstruction are explained by circles centered at the ends of the data set.

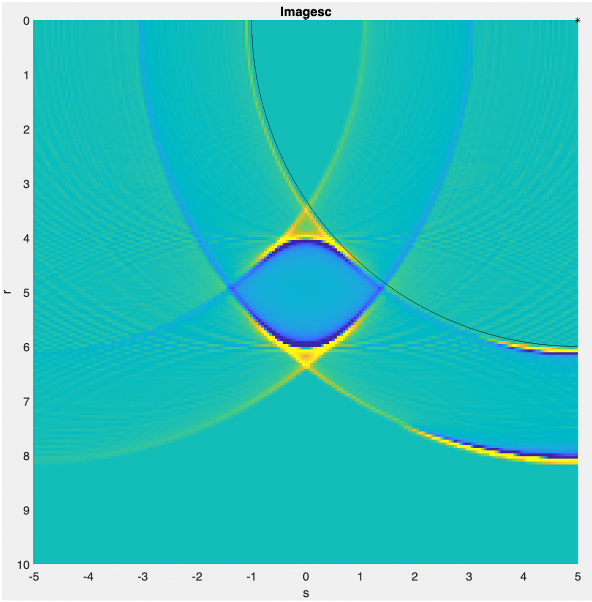

Figure 2: A circle centered at $(5, 0)$ plotted on top of the reconstruction artifact

The reconstruction method in problem one is imperfect, as it will often fail to reconstruct the left and right sides of the object, given where the source of the sonar waves is. Problem 2 implements a more advanced backprojection technique to help produce better reconstructions.

3. Problem 2. The second limited data tomography problem is similar to the first. It still uses limited data in both the centers and radii of the sonar waves. The difference is where the source of the sonar waves is. The source can now travel along any curve or line, not just along the ocean's surface. This means you can integrate over full circles instead of the semicircles used for the integration in problem 1 (see (2)). Now that the source of sonar waves can be along any curve, better reconstructions and new artifacts can be produced.

3.1. The Math Behind Problem 2. The math behind problem 2 is very similar to problem 1, with several subtle differences. The same characteristic function can be used as described in (1). In this problem, y_0 depends on the curve the sonar source travels on instead of being constantly 0. With these changes to the integral, the trapezoidal rule is used again to generate data on whether the circles being integrated over pass through the object. The same formula described in function (4) can be used to generate data on the central second difference. The same backprojection formula can also be used since the formula generalizes to curves other than the line along the ocean's surface:

The backprojection at a point $\bar{x}$ integrates data over all the circles in the data set that contain $\bar{x}$. If the sonar transceiver travels along the curve $\gamma(s)$, $\gamma : [a, b] \to \mathbb{R}^2$, and $\overline{x}$ is a point in the ocean, then the circle centered at $\gamma(s)$ through $\overline{x}$ has radius $\|\overline{x} - \gamma(s)\|$. The continuous backprojection of the function $g(\gamma(s), r)$ is

$$R^* g(\overline{x}) = \int_{s=a}^{b} g(\gamma(s), \|\overline{x} - \gamma(s)\|)\, ds, \qquad (6)$$

the integral of g over all circles in the data set (with centers $\gamma(s)$) that pass through $\overline{x}$. For problem 1, $\gamma(s) = (s, 0)$.

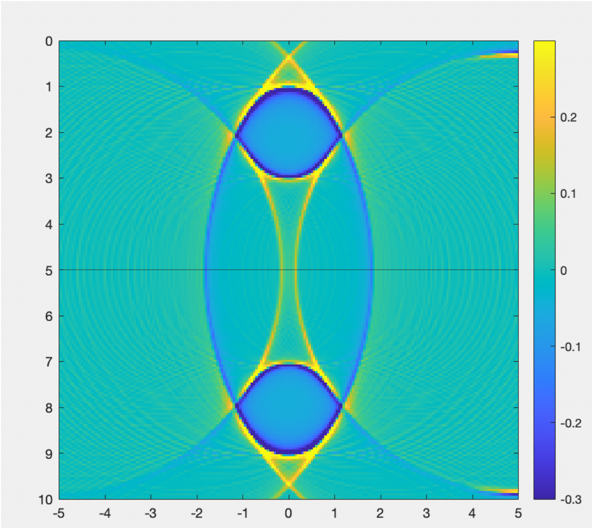

Figure 3: Reconstruction of a circle centered at $(0, 8)$ with radius 1 where the source of sonar waves is along the line $y = 5$. A reflection of the object is centered at $(0, 3)$.

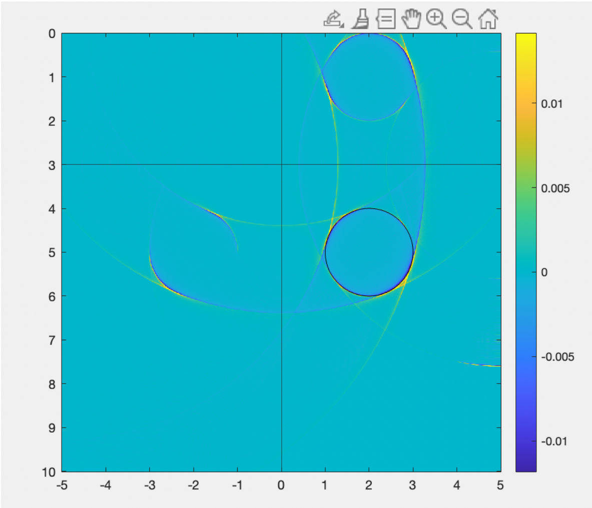

Figure 4: Reconstruction of a circle centered at $(2, 5)$ with radius 1 where the source of sonar waves is along the lines $y = 3$ and $x = 0$.

3.2. Reconstructions from Problem 2. The reconstruction in figure 3 produces more visible singularities than a reconstruction from problem 1 (i.e., figure 1). However, since the backprojection integration is symmetrical about the line of sources as the density is integrated over all of the circle, a reflection of the object is produced. The other artifacts in this reconstruction are from circles centered at the end of the data set, per principle 2.2. To resolve the issue of the reflection, one possibility is to have the sonar source travel along two paths. As illustrated in figure 4, it becomes clearer what object is being reconstructed; however, the object's reflections still exist. A better solution is to have the source of sonar waves travel along a curve, as the backprojection reconstruction does not produce any exact reflections of the object. Reconstructions where the sonar source travels along a curve produce artifacts that the above principles cannot explain.

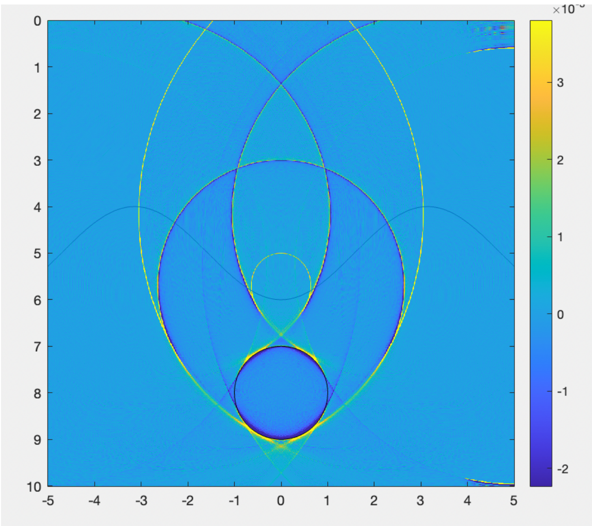

Figure 5: Reconstruction of a circle centered at (0,8) with a radius of 1 where the source of the sonar waves is along the curve $y = 5+\cos(x)$

3.3. Reconstructions Using Curves. As shown in figure 5, a circle reconstruction when the source of sonar waves is along the curve can yield a reconstruction with more visible singularities than when the source of sonar waves is traveling along a straight line. This is because more sonar wave circles are tangent to the object's boundary. The reconstruction in figure 5 produces some interesting artifacts. While the end of data set artifacts introduced in principle 2.2 still exist, they are faint compared to the other circular and non-circular artifacts in this reconstruction. The non-circular artifacts are significant to analyze because sonar wave circles would not produce them.

3.3.1. Artifact Analysis. The artifacts analyzed in this section will be the artifacts not produced by the end of the data set, namely the smaller teardrop shape in the center, the larger circle, and the symmetrical curves that are tangent to the object in figure 6. Most of these artifacts are explained by mirror points.

A mirror point is a point that is reflected over a particular line. Reflected points of points on the boundary of the object explain these artifacts. I will now describe how to find which lines the points are reflected over.

Figure 6 illustrates sonar wave circles centered on the curve and tangent to the object's boundary. The line that each point on the object is reflected over is the tangent line to the curve that passes through the center of the tangent circle. To find the mirror points mathematically, a point on the curve is first chosen. This point on the curve will act as the center of the tangent circle. To find the point on the object that the circle is tangent to, first, let $\bar{c}$ represent the center of the object and $\gamma(t)$ represent the point on the curve. The unit vector between $\bar{c}$ and $\gamma(t)$ is denoted:

$$\widehat{c\gamma(t)} = \frac{\gamma(t) - \bar{c}}{||\gamma(t) - \bar{c}||} \tag{7}$$

The unit vector described in function (7) is then scaled by the radius of the characteristic function in (1), R, so the vector is a normal vector of the circular object. The tangent points

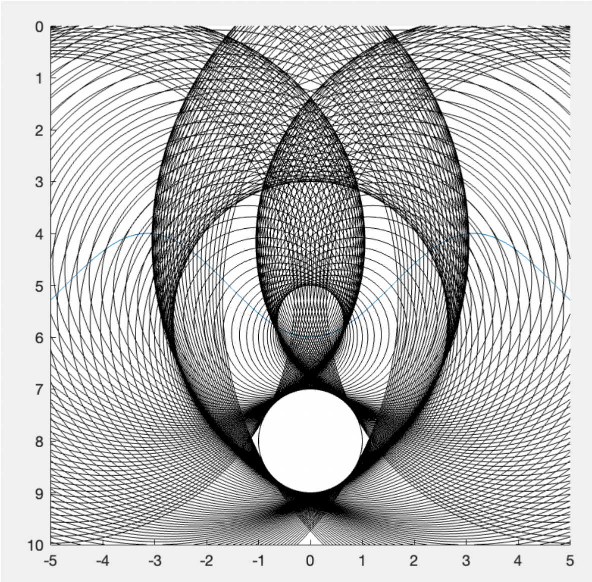

Figure 6: Circles centered on the curve $y = 5 + \cos(x)$ that are tangent to the boundary of the object.

on these circles are then described by:

$$\begin{aligned} &\bar{c} + R * \widehat{c\gamma(t)} \\ &\bar{c} - R * \widehat{c\gamma(t)} \end{aligned} \tag{8}$$

These points are then reflected over the tangent line, ℓ, to the curve, γ, at $\gamma(t)$. Let a be

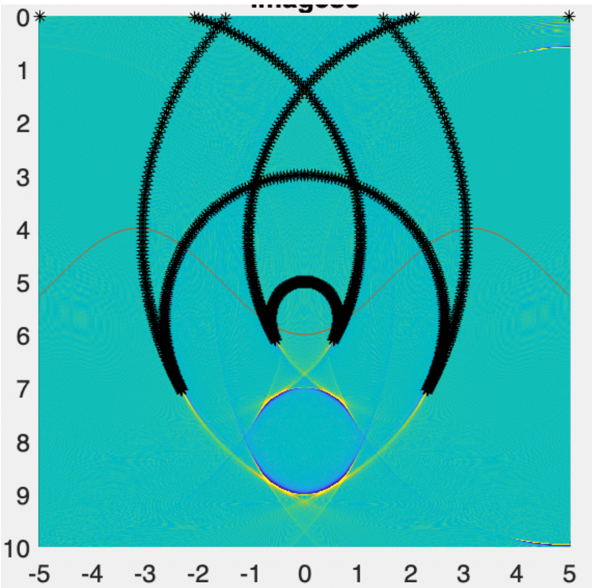

Figure 7: The mirror points of an object centered at (0,8) with radius 1 where the source of sonar waves is traveling along the line $y = 5 + \cos(x)$

one of these points on the object's boundary in (8) and let $\gamma(t)$ remain the same as described above. Let $\bar{v} = \bar{a} - \gamma(t)$. The goal is to reflect this vector over the tangent line to find the mirror point, which is done through the orthogonal vector projection. Let

$$\bar{\tau} = \gamma'(t)$$

be a direction vector of the tangent line. The scalar projection of $\bar{v}$ onto $\bar{r}$ is defined by:

$$\|\bar{v}\| * \cos(\theta) = \frac{\bar{v} \cdot \bar{\tau}}{\|\bar{\tau}\|} \tag{9}$$

where θ is the angle between $\overline{v}$ and $\overline{\tau}$ Let the vector $\overline{w}$ be the orthogonal projection of $\overline{v}$ onto the tangent line ℓ. The length of $\bar{w}$ is the scalar projection just calculated, so

$$\bar{w} = \frac{\bar{v} \cdot \bar{\tau}}{\bar{\tau} \cdot \bar{\tau}} * \bar{\tau} \tag{10}$$

and the perpendicular vector from ℓ to $\overline{a}$ is $\overline{v} - \overline{w}$. From here, the point $\bar{a}$ can be reflected over the tangent line to the point

$$\bar{q} = \overline{a} - 2 * (\overline{v} - \overline{w}) = -\bar{a} + 2 * (\gamma(t) + \bar{w}) \tag{11}$$

In this case, $\bar{q}$ represents the mirror point to $\overline{a}$, the reflection of $\overline{a}$ in the tangent line ℓ.

When all the mirror points are plotted, an image, as illustrated in figure 7, is produced.

The mirror points align with the artifacts not explained by principle 2.2. The mirror points cut off at around $r = 7$ because of the limited data from s or the possible centers of the circles. More artifacts generated by mirror points will be seen in the following reconstructions.

3.3.2. A New Artifact. Finally, in figure 5 there is one more set of artifacts that are not mirror point artifacts nor artifacts explained by principle 2.2. These artifacts appear at the boundaries of the circle being reconstructed and are highlighted in yellow in figure 7. These artifacts have yet to be justified mathematically, but they seem to derive from where all the tangent circles bunch together in figure 6. For this reason, these new artifacts are named stationary point artifacts. Our future research will involve analyzing these stationary point artifacts further to see if the theory about the derivation of these artifacts can be mathematically proven.

3.3.3. Developing an Optimal Reconstruction.
An "optimal" reconstruction would be where the object is reconstructed well (i.e., not many invisible singularities), and the number of artifacts is minimized. The artifacts that do appear should be easy to explain. One of the curves that generate an optimal reconstruction is a parabolic curve where the object is centered around the parabola's focus.

In figure 8, the square is reconstructed almost entirely with visible singularities, and the artifacts above the parabolic curve are end of data set artifacts. The square's boundaries are primarily visible singularities because centering the square allows many sonar wave circles to be tangent to it. The artifacts below the parabolic curve are mirror point artifacts. With this condition, objects centered around the focus of a parabola have generated the best possible reconstructions so far.

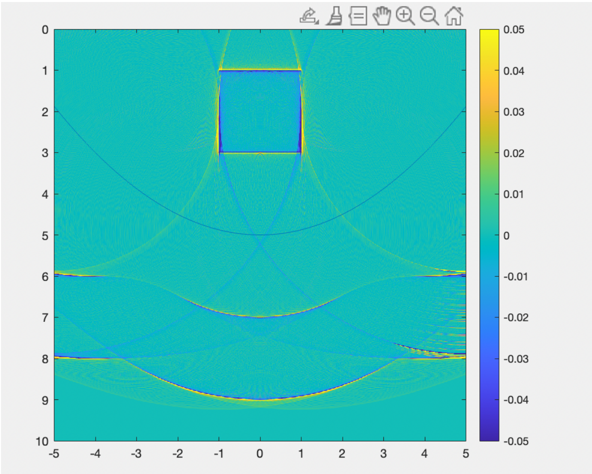

Figure 8: A reconstruction of a square centered at (0,2) where the sonar source is traveling along the line $y = 5 - 1/8 * x^2$

4. Conclusions.

In our research, we have verified end-of-data set artifacts for a different limited data tomography problem. We also demonstrated that mirror point artifacts exist in image reconstructions. Finally, we found a new type of artifact, stationary point artifacts, in our reconstructions. We were able to begin to explore what type of curves the sonar source should travel on to develop optimal reconstructions.

4.1. Further Research.

In the future, we would like to mathematically prove the theory about where the stationary point artifacts are coming from. Further, we would like to explore reconstructing different shapes more, and we would also like to see if reconstructing a different shape affects what curve the sonar source should be traveling along to develop an optimal reconstruction.

5. Acknowledgements.

I would like to thank Dr. Todd Quinto for his fantastic mentorship during the VERSEIM REU program at Tufts University. I would also like to thank the NSF for providing the funding to make this research possible through NSF REU grant DMS 2050412.

REFERENCES

[1] M. Agranovsky and E.T. Quinto, Injectivity sets for radon transform over circles and complete systems of radial functions, J.Functional Anal., 139 (1996), pp. 383–414.
[2] L. Borg, J. Frikel, J.S. Jørgensen, and E.T. Quinto, Analyzing reconstruction artifacts from arbitrary incomplete X-ray CT data, SIAM J. Imaging Sci., 11 (2018), pp. 2786–2814.
[3] R. Courant and D. Hilbert, Methods of Mathematical Physics, vol. II, Wiley-Interscience, New York, 1962.
[4] J. Frikel and E.T. Quinto, Artifacts in incomplete data tomography with applications to photoacoustic tomography and sonar, SIAM J. Appl. Math., 75 (2015), pp. 703–725.
[5] V.P. Krishnan and E.T. Quinto, Microlocal analysis in tomography, in Handbook of Mathematical Methods in Imaging, O. Scherzer, ed., Springer Reference, Springer, 2015, pp. 847–902.
[6] F. Natterer and F. Wübbeling, Mathematical Methods in Image Reconstruction, Monographs on Mathematical Modeling and Computation, Society for Industrial and Applied Mathematics, New York, 2001.

[7] L. V. Nguyen, How strong are streak artifacts in limited angle computed tomography?, Inverse Problems, 31 (2015), p. 055003.
[8] ———, On artifacts in limited data spherical radon transform: flat observation surfaces, SIAM J. Math. Anal., 47 (2015), pp. 2984–3004.
[9] E.T. Quinto, Singularities of the X-ray transform and limited data tomography in $\mathbb{R}^2$ and $\mathbb{R}^3$, SIAM J. Math. Anal., 24 (1993), pp. 1215–1225.
[10] E.T. Quinto, Artifacts and visible singularities in limited data x-ray tomography, Sensing and Imaging, 18 (2017).
[11] W. Symes, Mathematics of Reflection Seismology, tech. report, Rice University, 1998.